RP Current Trends In Applied Sciences
Vol. 1, No. 1 (October – December 2022) pp. 5–10
e-ISSN: 2583-7486

RESEARCH PLATEAU PUBLISHERS

Cite this article: J. Gahlawat, Time-dependent perturbation treatment for free induction decay and dynamic Stark effect in semiconductor quantum wires, *RP Cur. Tr. Appl. Sci.* **1** (2022) 5–10.

Original Research Article

Time-dependent perturbation treatment for free induction decay and dynamic Stark-effect in semiconductor quantum wires

Jyoti Gahlawat
Department of Physics, Baba Mastnath University, Asthal Bohar, Rohtak – 124021, Haryana, India
*Corresponding author, E-mail: jgahlawat.bmu@gmail.com

ARTICLE HISTORY
Received: 27 August 2022
Revised: 19 October 2022
Accepted: 21 October 2022
Published online: 23 October 2022

KEYWORDS
Time-dependent perturbation treatment; Stark effect; free induction decay; semiconductor quantum wires.

ABSTRACT
The analysis of the occurrence of coherent optical transient processes in direct-gap semiconductor quantum wires with thickness and width less than the bulk Wannier-Mott exciton Bohr radius is covered in this study. These processes include the dynamic Stark effect and free induction decay. A relatively strong magnetic field's contribution to the occurrence of transient processes has been investigated. The analysis is based on the near band gap resonant excitation regime time dependent perturbation treatment of the coherent radiation-semiconductor interaction model. Lower than the Mott transition phase, the excitation intensity is maintained. Calculations show that the magnetic field has a significant impact on the Stark shift, Stark broadening, and free induction decay of a GaAs/AlGaAs quantum wire exposed to femtosecond pulses from a Ti:Sapphire laser. Furthermore, Stark splittings are also influenced by wire width.

1. Introduction

In nonlinear spectroscopy, an important field of study is the investigation of optical coherent transient processes. These transient processes, which take place on time scales in which the excitation duration is substantially smaller than the decay durations, include, among other things, the nonlinear optical processes known as optical nutation (ON), free induction decay (FID), dynamic Stark effect (DSE), and Rabi oscillations (ROs). One can comprehend the pathways for stimulation energy transitions among levels and also the interactive characteristics of resonant transitions by carefully analysing coherent transients.

Theoretical research and practical observation of optical coherent transient processes in atomic and sub-atomic systems started around 1970s [1]. It is widely recognised that the semiconductor media, such as substances or composites including polycrystalline materials, always had the tremendous scientific potential for the manufacture of reduced dimensional lasers and photonic diffraction gratings which are useful in optoelectronic information transfer, and also femtosecond optoelectronic equipment such as switching devices and storage components. In contrast to the dephasing periods for atomic systems, which are measured in microseconds, these crystals exhibit femtosecond-level dephasing periods, which are incredibly low. Coherent transient response in semiconductor materials may now be studied thanks to the advancement of ultrafast pulse continuous laser around 1980s.

The advancements in femtosecond laser technology and sophisticated material production methods like MOCVD, MBE, LPE, and VPE should make it possible to successfully observe coherent transient processes in bulk materials and also virtual quantum well structure in two dimensions [2]. The bounded *e-h* pairs, also named as excitons, are extremely important for an investigation of the optical absorption spectra of semiconductors. It's noteworthy to observe that the excitonic effect is greatly enhanced when the material dimension is decreased from 3 to 2. Researchers were inspired to further limit the structure using 3- or 2-dimensional confinements, leading to the development of materials known as quantum dots (QDs) and quantum wires (QWRs) which are basically zero- and one-dimension structures, respectively. In the scenario of current research, attention has been focused in understanding the mechanisms behind the nonlinear optical processes and the characteristics of the materials mentioned above, namely QWRs and QDs, which have promising future applications in nano-optics [2, 3].

The spectral characteristics of the nonlinear optical media are significantly affected by their magnetization, resulting a triple implication on the propagation features via Landau threshold dissociation, contrast enhancement of density-of-states, and alteration of the hydrogen atom like quasi boson-exciton wave-function [4, 5].

The aforementioned events served as the inspiration for the current discussion. The analytical analysis of two optically excited transient effects in a single QWR, viz. the free induction decay (FID) and the dynamic Stark effect (DSE) both with and without a fairly strong magnetisation, is the aim of this research work. Here, it should be underlined that the introduction of a relatively strong magnetostatic field can improve and modulate the optical characteristics of the QWRs [6]. In the near band gap resonant transition region, numerical

estimates of the dynamic Stark effect and free induction decay have been made for GaAs/AlGaAs that have been properly shone by femtosecond pulsed Ti:Sapphire lasers. The findings qualitatively match the experimental data that is currently available.

2. Theoretical formulations

Since the excitonic energy level in direct-gap semiconducting materials with lattice distortion Wannier-Mott discrete excitonic structural system is presumed toward being nearer to resonance with the pump photon energy level in the present research of the interaction among both ultra-short pulsed coherent irradiance and semiconducting materials, the author has employed the time-dependent perturbation approach. The author exclusively analyse the lowest excitonic energy state (i.e., for n = 1, 1s-state) for the realm of low to medium excitation intensity. The (highest) valence band and the (lowest) conduction band may be regarded to be the only places where photo-induced electronic changes can take place. Near the Brillouin zone's centre, these bands may be regarded to possess parabolic structure, non-degenerate, and isotopic with an electron wave vector $|\vec{k}| \sim 0$. The crystal's lower state represented by $|a\rangle$ and the excited *e-h* pair state represented by $|b(\vec{k})\rangle$ are the states (or levels) between which the photo-induced inter-band transitions occur. The relevant transition energy $|b(\vec{k})\rangle$ (at the energy state) may be expressed as:

$$\hbar\Omega_k = \hbar\Omega_{g,eff} + \frac{\hbar^2 k^2}{2m_r} + i\hbar\gamma_{inh}\,. \tag{1}$$

Here, the author presumed that the wire length is in the lateral direction, as seen in $k_y^2 = k^2$. Whereas

$$k_{z,x} = \frac{\pi j_{z,x}}{L_{z,x}} \quad \text{where} \quad j_{z,x} \in N\,;$$

stands for QWR's size along either the z or z-axis. The author has assumed that the thin QWRS Bohr radius is smaller in comparison to the bulk excitonic Bohr's radius a_{ex}. The diminished *e-h* pair mass m_r is also present. The term $i\hbar\gamma_{inh}$ in Eq. (1) has been used to phenomenologically introduce the influence of inhomogeneous broadening originating via different intrinsic disordered mechanisms including flaws, pollutants, and size non-uniformity in the QWR. We've established:

$$\Omega_{g,eff} = \Omega_g + \frac{\hbar^2 k^2}{2m_r}(L_x^{-2} + L_z^{-2})\,; \tag{2}$$

$\hbar\Omega_g$ is bandgap energy of bulk crystal. Eq. (1) takes the general form when moderately magnetized under the influence of magnetic field *B*:

$$\hbar\Omega_{Bk} = \hbar\Omega_k + \frac{\hbar\Omega_c}{2} + (g_c - g_v)\beta B M_j \tag{3}$$

where $\Omega_c = |eB/m_r|$, β is the Bohr's magniton, $g_{c,v}$ stands for Lande' g-factor, and $M_j = 1/2$. For applications requiring moderately high magnetic fields, the author only took the lowest Landau levels into account while creating Eq. (3). Coulomb interaction significantly modifies the material's optical response for a relatively thin quantum wire [7], which justifies its inclusion in the motion's equations. Under RWA, the probability amplitude of ground and excited state of crystal under the limited magnetic field are, respectively, given as [8]:

$$i\hbar\dot{a} = \frac{1}{2}\sum_k \mu_{ba} E_0 \exp[-i(\Omega_{Bk} - \Omega)t] b(\vec{k}) \tag{4}$$

and

$$i\hbar\dot{b}(\vec{k}) - \sum_{k'} \langle \vec{k}|U|\vec{k}'\rangle \exp[i(\Omega_{Bk} - \Omega_{Bk'})t] b(\vec{k}') = -\frac{1}{2}\mu_{ab} E_0 \exp[i(\Omega_{Bk} - \Omega)t] a - \hbar\Gamma b(\vec{k})\,, \tag{5}$$

It is considered that the electric dipole moment operator represented by $\langle b|\hat{\mu}|a\rangle$ behaves in a manner in the direction of electric field $\vec{E}(t) = (0.5)E_0 \cos\Omega t$ being applied, and the author has also assumed that the interaction Hamiltonian takes the form of dipole. In Eq. (5), $\Gamma = \gamma + \gamma_{inh}$; $\gamma = T_2^{-1}$; T_2 is the de-phasing time. The phrase, which is defined as the Coulomb interaction energy $\langle \vec{k}|U|\vec{k}'\rangle$ and provided by

$$\langle \vec{k}|U|\vec{k}'\rangle = -\int \exp[-(k-k')y] \frac{e^2}{(y_0 + |y|)\varepsilon} dy \tag{6}$$

with $\varepsilon = \varepsilon_0\varepsilon_l$ and $y_0 \geq 0$ is introduced as a cut-off. The answers to the equations for $a(t)$ as well as $b(k,t)$ may be found by using a common methodology [8] as follows:

$$a(t) = [\cos\theta - i(X/\beta)\sin\theta]\exp(iXt/2) \tag{7}$$

and

$$b(k,t) = i\mu_B E_0/\hbar\beta)\left|\psi_{1B}(o)\right|^2 \sin\theta.\exp[i(\omega_{Bk} - \omega + X/2)t \tag{8}$$

where $\theta = \beta t/2$, $\beta^2 = X^2 + 4\Omega_{exR}^2$, $\Omega_{exR} = |\mu_B E_0/2\hbar|\psi_{1B}(o)$, $X = \Delta_B + i\Gamma$, $\Delta_B = \Omega - \Omega_{B1}$, $\hbar\Omega_{B1} = \hbar\Omega_B - [\varepsilon_{ex}(0)]_{ld}$, $\Omega_B = \Omega_{g,eff} + \Omega_c/2$, $|\mu_{ba}| = |\mu_{ab}| = \mu_B$, and $\psi_{1B}(0)$ is the hydrogenic excitonic wave-function corresponding to the 1*s* excitonic state under the action of magnetising field *B*. To prevent the resulting singularity, the excitonic binding energy (EBE) $[\varepsilon_{ex}(0)]_{ld}$ in the quantum wire must be chosen from the empirically calculated values for the particular geometrical dimension [9]. When a magnetising field is present, EBE is defined as:

$$\varepsilon_{ex}(o) = 3\left[\frac{\hbar eB}{2(2n+1)m_r R^*}\right]^{1/2} R^* D \tag{9}$$

with D = 1 for the quantum wire structure and R^* stand for the bulk EBE. The variational approach is used to obtain the n = 1, $\psi_{1B}(o)$ is exciton wavefunction, which is then addressed in later section. Using Eqs. (7) to (9), one is enable to investigate crucial nonlinear optical processes (in the time domain) in thin

semiconductor QWBS under both the appearance as well as non-appearance of magnetising field, including ON, DSE, and FID. The author only focused on SDE and FID in this paper. The author solved Eq. (4) to get the expressions for the Stark broadening S_{eB} and the Stark shift S_B in the magnetized QW quantum wire for the 1s excitonic state, and then use these values to explore the dynamic Stark effect.

$$S_B = \frac{\Omega_{exR}^2 \Delta_B}{(\Delta_B^2 + \Gamma^2)} \tag{10a}$$

and

$$S_{eB} = \frac{\Omega_{exR}^2 \Gamma}{(\Delta_B^2 + \Gamma^2)}. \tag{10b}$$

These equations demonstrate how the magnetising field, the EBE, and the wave-function all affect the Stark effect via Landau level splitting. The following section outlines the theoretical characteristics of S_{eB} and S_B in terms of the magnetising field. The following can be done to understand the other significant nonlinear optical (time dependent) process, known as FID, in the magnetised QWR. The author supposed that during the optical laser pulsing period, or time $t = 0$ to t_p, the femto-second pulsed laser illuminates the chosen media. The free induction decay pulse is obtained at periods $t > t_p$ and at $t' = t - t_p = T_2^*$, the dephasiing time, when a pulsing is shut off and the strength of the pulse is $1/e^2$ that at $t = t_p$.

The values of the parameters a and $b(k)$ at $t = t_p$, obtained via Eq. (7) and Eq. (8), and $t'(= t - t_p) > 0$ and also the fundamental picture may be used to determine the induced polarisation $P(t')$ in the free induction decay regime:

$$P_B(t') = N_B \left\langle \mu_B(t') \right\rangle \tag{11}$$

with

$$\left\langle \mu_B(t') \right\rangle = \mu_B [a(t') \sum_k b^*(k,t') \exp(i\Omega t') + c.c.]. \tag{12}$$

The *e-h* pair's concentration in the magnetised QWR, denoted via N_B in Eq. (11), is given by

$$N_B = \frac{eBL_xL_yL_z}{4\pi^2\hbar} \Delta k_y; \tag{13}$$

Δk_y is a little shift in the direction of the electron wave along the quantum wire length. The following is [11]:

$$P_B(t') = \frac{2N_B \mu_B^2 E_0}{\hbar|\beta|^2} |\psi_{1B}(o)|^2 \times \left[X \sin^2\left(\frac{\beta t_p}{2}\right) + i\beta \cos\left(\frac{\beta t_p}{2}\right) \sin\left(\frac{\beta^* t_p}{2}\right) \right] \times \exp(iXt_p).\exp[i(\Omega_{B1} + i\Gamma)t']. \tag{14}$$

While calculating $P_B(t')$ for onset of optical pulse-semiconductor quantum wire interactions system, one should be cognizant of the wave-function for the 1s excited-state in QW in real space in addition to the other physical properties. The author constructed the excitonic trial wave function using the traditional variational method, much like the model developed in Ref [10].

$$\psi = g_t(x,\eta)\chi_e(z_e)\chi_h(z_h)\phi_e(y_e)\phi_h(y_h); \tag{15}$$

$g_t(x,\eta)$ is the orbital function of type Gaussian given as:

$$g_t(x,\eta) = \left(\frac{2}{\pi}\right)^{1/4} \frac{1}{\sqrt{\eta}} \exp\left[-\left(\frac{x}{\eta}\right)^2 \right]. \tag{16}$$

In Eq. (16), η is the parameter that controls the *e-h* pair separation in Eqs. (15) and (16). The wave function's z component, which is unaffected by the magnetic field, is the variable $\chi_{e,h}(z_{e,h})$. Assuming that the situation is equivalent to that of a particle in 1-d box, it may be assumed that

$$\chi_{e,h}(z_{e,h}) = \left(\frac{2}{L_z}\right)^{1/2} \cos\left(\frac{z_{e,h}\pi}{L_z}\right). \tag{17}$$

Using the eigen-value equation, *e-h* pair wave-functions $\phi_{e,h}(y_{e,h})$ are numerically determined in the transverse direction as:

$$\frac{\partial^2\phi(y)}{\partial y^2} + \frac{2m_r}{\hbar^2} E\phi(y) - \left(\frac{y}{l_B^2}\right)\phi(y) + 2\frac{y}{l_B^2}k_x\phi(y) - k_x^2\phi(y) = 0. \tag{18}$$

In Eq. (18), $l_B = \sqrt{\hbar/eB}$. The solution of Eq. (18) yields:

$$\phi(y) = C\cos(K_y y), \tag{19}$$

where $C = \left(\frac{2}{L_y + \sin(K_y L_y)/K_y} \right)^{1/2}$

and

$$K_y^2 = \frac{2m_r E}{\hbar^2} - \left(\frac{y}{l_B^2} - k_x\right)^2.$$

In order to maintain the nonparabolicity effect, the greatest value for k_x that can be used to determine the length of the wire that should be used is provided by [3]:

$$\frac{y}{l_B^2} << 2.5\times10^8 \text{ m}^{-1}. \tag{20}$$

It is significant to notice that the trial wave-function corresponding to the condition: $L_x, L_z < 3a_{ex}$ [6], implicitly pre-supposes that the holes and the electron are separately confined along the lateral and the transverse directions. The relation can be used to compute the time dependent transmission intensity (for $t' > 0$).

$$I_{TB}(t') = \frac{1}{2}\varepsilon c_l \left|E_{TB}(t')\right|^2 \quad (21)$$

with

$$\left|E_{TB}(t')\right| = \frac{i\omega L_y}{2\varepsilon c_l} P_B(t') \,. \quad (22)$$

In above equations, c_l stands for pulse speed in the semiconductor QWR.

3. Results and discussion

3.1. Un-magnetized semiconductor QWR

We have taken into account the *e-h* pair density sufficiently smaller than a particular value named as Mott density N_B = 0. Here, it should be noted that for *e-h* pair's density greater than the Mott density, the exciton influences are screened and *e-h* plasma effect justifies its incorporation, in order to study FID in semiconductor quantum wire in the non-appearance of magnetizing field. The author has assumed $N_{B=0} = 8\times10^7$ m^{-1} for a quantum wire of GaAs/AlGaAs, as Rossi and Molinari [12] did in their research analysis. The analytical computations of free-induction decay in the GaAs/AlGaAs quantum wire at the temperature of 5K having dimension of $L_x = L_z = 0.56a_{ex}$, where the bulk excitonic Bohr radius is set to 120 angstroms, are presented here. It is envisaged that a Ti: Sapphire laser emitting optical pulses of duration t_p > 120 femto-second and a time-resolution of 50 femto-second will be used to irradiate the QWR. Nonlinear optical (time dependent) processes such as photon echo and FID have already been shown in time-resolved studies with a precision of 50 fs in GaAs quantum wells [13]. The additional material's characteristics are: $\hbar\omega_g = 1.52$ eV, $\varepsilon_l = 12.56$, $m_r = 0.0614m_0$, $\gamma = 4.55\times10^{12}$ s^{-1}, $\gamma_{inh} = 9\times10^{11}$ s^{-1}, $\varepsilon_{ex}(o) = 6.0$ meV, $\mu_{B=0} = 9.78\times10^{-29}$ Cm. Figures 1 - 4 displays the numerical analysis's findings.

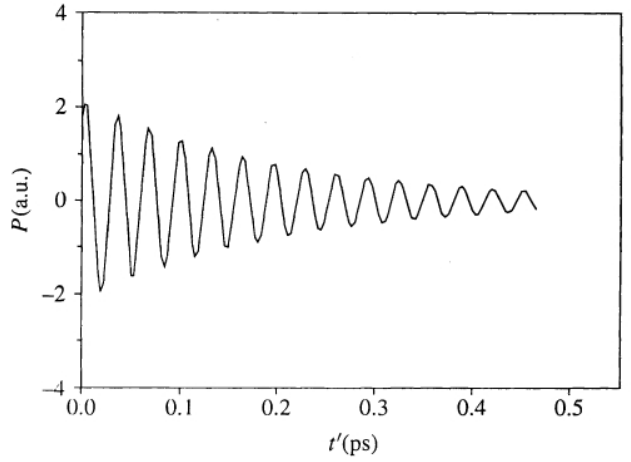

Figure 1. The change in transient polarisation P with time t' in a GaAs/$Ga_{0.4}Al_{0.6}$As QWR during the decay phase.

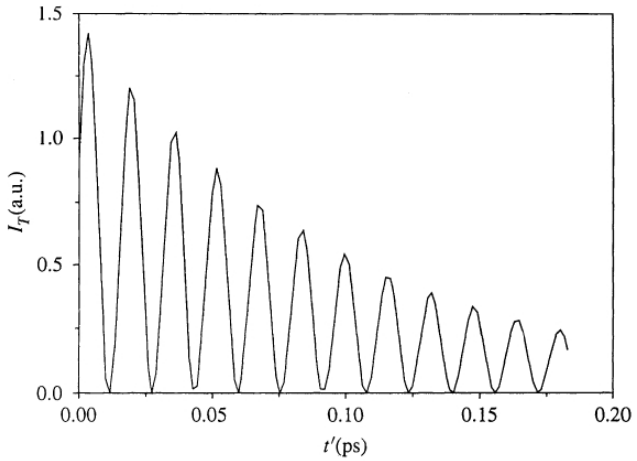

Figure 2. The transient transmitted intensity I_T's decay curve (versus time t') in the GaAs/$Ga_{0.4}Al_{0.6}$As QWR arrangement.

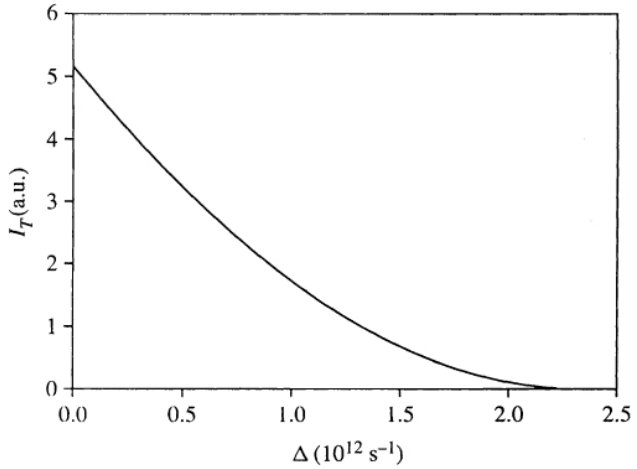

Figure 3. Nature of transmitted intensity I_T dependency regarding the detuning Δ in the GaAs/$Ga_{0.4}Al_{0.6}$As QWR structure.

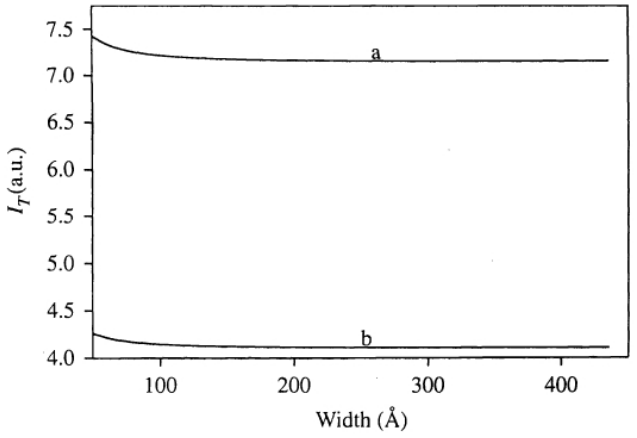

Figure 4. Nature of dependence of transmitted intensity in GaAs/$Ga_{0.4}Al_{0.6}$As QWR structure in QWR width L_x. Curves (a): L_z = 7.5 nm and Curve (b) L_z = 10 nm.

Figures 1 and 2 show how the transmitted intensity I_T and polarisation P change over time in the decay state for t' > 0 later than the pulse has passed in the non-appearance of the magnetization (Eq. 21). In Figure 1, the polarisation shows ringing behaviour that degrades progressively. The transmitted

signal's FID is visible in Figure 2. The author has now examined the characteristics of the breakdown of FID pulse in order to determine the sort of free induction decay that is occuring, specifically whether it is 1st or 3rd order FID. The author made an assumption that the laser-semiconductor system may sustain inhomogeneous broadening in order to keep the analysis comparatively straightforward.

The photo-induced *e-h* pair density can be seen as being insufficiently big under a moderate excitation limit in order to prevent saturation and prevent the nonlinear third-order free induction decay from becoming important. As a result, the author has limited their attention to 1st order FID research in direct bandgap semiconductor QWRs. Remember that 1st-order FID process simply vanishes in the duration $T_2^* < T_2$, the dephasiing time. The author used $T_2 = 0.217$ ps for analytical computation of 1st order FID in GaAs/AlGaAs quantum well structures and predicted that the signal would disappear after 0.1 ps. It is assumed that the pulse lasts for 0.1 ps. The above illustration demonstrates that the created free induction decay signal increases by $1/e^2$ times its starting limit in less duration than $T_2 = 0.217$ ps, or $T_2^* \sim 0.19$ ps. The 1st order FID pulse in two-level systems decreases to $1/e^2$ of its starting limit within a dephasing duration T_2^* [14], supporting the author's findings. As a result, one may estimate the time duration T_2^* from Figure 2 as well as conclude that 1st order FID in GaAs/$Al_{0.6}Ga_{0.4}$As QWR is observable. Additionally, an intensity that is delivered has a ringing quality.

Figure 3 shows the transmission intensity I_T with regard to detuning value $\Delta = \omega - \omega_1$. It is clearly understood that the peaks occur under resonance conditions and decline as one approach off-resonance conditions. Since the decay constant is larger and jointly the decay profile is established, the oscillatory behaviour is hidden in this case.

The behaviour of transmitted intensity in GaAs/$Ga_{0.4}Al_{0.6}$As QWR structure in QWR width L_x is depicted in Figure 4. Here, curves *a* and *b* stand for the features for $L_x = 75$ angstrom and $L_x = 100$ angstrom, respectively. The findings are in strong qualitative agreement with those found in Ref. [15], where it was shown how the absorption coefficient varied depending on the cross-section of the wire. Figure 4 also shows that both curves significantly decline for smaller dimensions before reaching a nearly steady value at 150 angstrom. This happens because as wire width increases, electrostatic confinement diminishes, causing the binding energy to drop as well. Due to insufficient confinement along the z-direction, when L_x increases beyond 150 angstrom, it comes closer to the bulk value rather than the 2D limit.

3.2. Magnetized semiconductor QWR

In Figure 5, the author has presented the nature of dependence of excitating field (E) of the Stark broadening as well as Stark shift for two different values of magnetized field strength. As opposed to Stark broadening, which fluctuates rather gradually with increasing magnetic field, the graphic clearly illustrates the dramatic dependency of Stark shift on magnetising field. Additionally, one can demonstrate how an increase in wire width dramatically improves the Stark shift. These wire width and magnetic field dependencies on Stark splitting are consistent with the findings in Ref. [6].

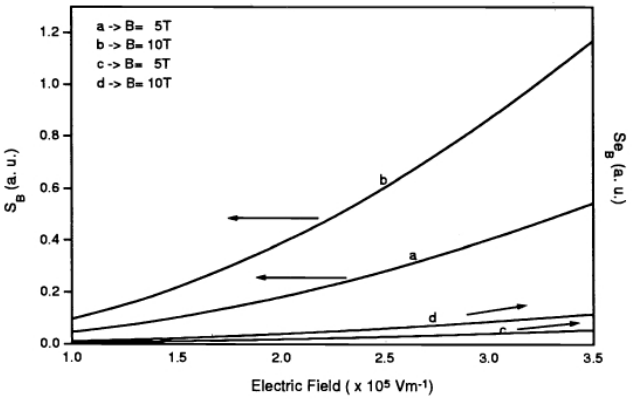

Figure 5. Stark broadening and Stark shift variations for two separate magnetic fields. $L_{x,z} = 10$ nm in a GaAs/AlGaAs QWR as functions of electric field.

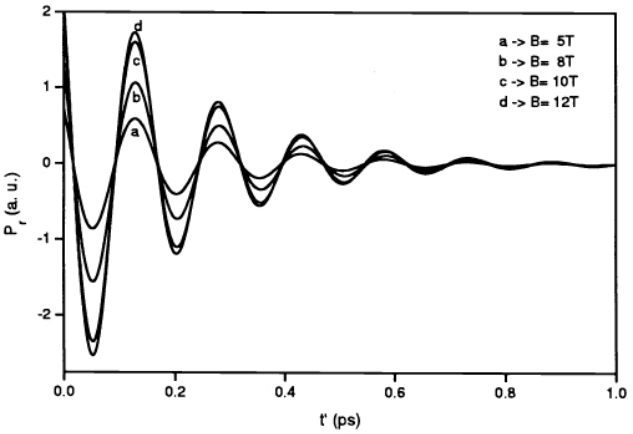

Figure 6. Temporal dependence of real component of induced polarisation in the appearance of magnetising field in a GaAs/AlGaAs QWR with width $L_{x,z} = 10$ nm.

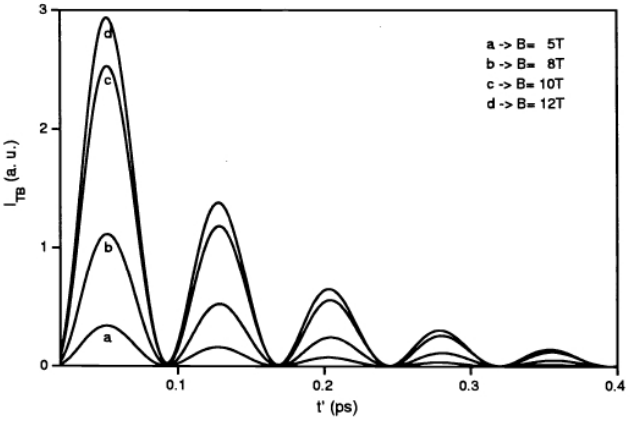

Figure 7. Time dependence of transmitted intensity in a GaAs/AlGaAs QWR that is 10 nm wide and operating in various magnetic fields.

In Figures 6 and 7, the author has shown the nature of real component of polarisation P_r and (time dependent) transmitted intensity $I_{TB}(t')$ under free induction decay regime, respectively. From Figure 6, the oscillatory decrease in $P_r(t')$ is about to occur. It should be noted that the dephasing duration T_2 is longer than the free induction decay signal's reduction to $(1/e^2)$ times its maximum value as obtained in Figure 7 ($T_2^* \sim$

0.17 pico-seconds). The sharpness of periodic properties of decay pulses is increased by growing magnetic field.

4. Conclusions

This study examines the existence of DSE and FID in semiconductor QWRs having dimensions lesser in comparison to the bulk Wannier-Mott exciton Bohr radius. The influence of the moderate magnetizing field in transient processes is investigated. The investigation is based on the nonlinear optical laser-semiconductor interaction model's time-dependent perturbation approach of the bandgap resonant excitation region. The excitation intensity is preserved lower than the Mott transition phase. The Stark shift, Stark broadening, and FID of GaAs/AlGaAs QWR illuminated by femtosecond laser pulses can all be significantly influenced by the magnetic field, according to calculations. Furthermore, wire width has an impact on Stark splittings.

References

[1] L. Allen, J.H. Eberly, Optical Resonance and Two-Level Atoms, John-Wiley, New York (1975).

[2] P. Peyhgambarian, S.W. Koch, A. Mysyrowicz, Introduction to Semiconductor Optics, Prentice-Hall, New Jersy (1993) pp. 235-245.

[3] J.H. Davies, Physics of Low-Dimensional Semiconductors, Cambridge University Press, Cambridge (1998) pp. 219-236.

[4] S. Bhan, S.P. Singh, V. Kumar, M. Singh, Low threshold and high reflectivity of optical phase conjugate mode in transversely magnetized semiconductors, *Optik* **184** (2019) 464-472.

[5] S. Glutsch, D.S. Chemla, Transition to one dimensional behavior in the optical absorption of quantum-well wires, *Phys. Rev. B* **53** (1996) 15902.

[6] L. Fedichkin, A. Fedorov, Study of temperature dependence of electron-phonon relaxation and dephasing in semiconductor double-dot nanostructures, *IEEE Trans. Nanotech*. **4** (2005) 65-70.

[7] H. Ando, H.O. Oohashi, H. Kanbe, Carrier-induced optical nonlinear effects in semiconductor quantum well wire structure, *J. Appl. Phys*. **70** (1991) 7024-7032.

[8] S. Banerjee, P.K. Sen, Optical coherent transient effects in a magnetized semiconductor quantum wire, *Superlatt. Microstr*. **29** (2001) 347-358.

[9] L. Banyai, I. Galbaith, C. Ell, H. Haug, Excitons and biexcitons in semiconductor quantum wires, *Phys. Rev. B* **36** (1987) 6099-6104.

[10] M.G. Barseghyan, A.A. Kirakosyan, D. Laroze, Laser driven interband optical transitions in two-dimensional quantum dots and quantum rings, *Opt. Commun*. **383** (2017) 571-576.

[11] A.L. Mese, The normalized transition energies between ground (1s) and first excited (1p) states in a GaAs/$Ga_{1-x}Al_xAs$ spherialquantum dot (SQD), *Superlatt. Microstr*. **156** (2021) 106932.

[12] F. Rossi, E. Molinary, Coulomb-induced suppression of band-edge singularities in the optical spectra of realistic quantum wire structures, *Phys. Rev. Lett*. **76** (1996) 3642-3645.

[13] G. von Plessen, T. Meier, M. Koch, J. Feldmann, P. Thomas, S.W. Koch, E.O. Gobel, K.W. Goossen, J.M. Kuo, R.F. Kopf, Exciton ionization induced by electric field in a strongly-coupled GaAs/AlGaAs superlattice, *Phys. Rev. B* **53** (1996) 13688.

[14] M.D. Levenson, S.S. Kano, Introduction to Nonlinear Laser Spectroscopy, Academic Press, San Diego (1988).

[15] D.L. Crawford, R.L. Nagarajan, J.E. Bowers, Comparion of bulk and quantum wire photodetectors, *Appl. Phys. Lett*. **58** (1991) 1629-1631.